

~~SECRET~~

UNCLASSIFIED

NACA RM E57C18

3.5.2.2
3.12.1.4
3.4.8.2

P.1



RESEARCH MEMORANDUM

EXPERIMENTAL EVALUATION OF "SWIRL-CAN" ELEMENTS
FOR HYDROGEN-FUEL COMBUSTOR

By Warren D. Rayle, Robert E. Jones, and Robert Friedman

Lewis Flight Propulsion Laboratory
Cleveland, Ohio

**CLASSIFICATION CHANGED
TO UNCLASSIFIED**

CLASSIFICATION CHANGED PER ADH. OF NASA 'DQ. MEMO

DTD 8-21-71, s.H. G. Haines,
C.E.J. 8-7-72

~~CONFIDENTIAL~~

To _____

By authority of NASA PA#7, Date June 2, 1959
effective date May 29, 1959. *by JBE*

I.N. 11,394

MAY 14 1957

CLASSIFIED DOCUMENT

This material contains information affecting the National Defense of the United States within the meaning of the espionage laws, Title 18, U.S.C., Secs. 793 and 794, the transmission or revelation of which in any manner to an unauthorized person is prohibited by law.

NATIONAL ADVISORY COMMITTEE FOR AERONAUTICS

WASHINGTON

May 13, 1957

N A C A LIBRARY

LANGLEY AERONAUTICAL
Langley Field, Va.

~~SECRET~~ UNCLASSIFIED
~~CONFIDENTIAL~~



UNCLASSIFIED
NATIONAL ADVISORY COMMITTEE FOR AERONAUTICS

RESEARCH MEMORANDUM

EXPERIMENTAL EVALUATION OF "SWIRL-CAN" ELEMENTS
FOR HYDROGEN-FUEL COMBUSTOR

By Warren D. Rayle, Robert E. Jones, and Robert Friedman

SUMMARY

The performance of "swirl-can" combustor elements for an experimental short-length turbojet combustor utilizing hydrogen fuel was studied at high-altitude operating conditions. Fuel was injected into each element through a tangential, sonic orifice that created a swirling fuel-air mixture within each element. The elements varied from 1.5 to 2.5 inches in length and from 1.3 to 2.0 inches in diameter and served as combined fuel injectors and flame stabilizers. Combustion efficiency of the individual elements exceeded 70 percent at a reference velocity of 180 feet per second, a pressure of 5.7 inches of mercury absolute, and an inlet temperature of 350° F in a combustor length of about 13.5 inches. Conical and cylindrical elements with an inlet that was covered with an orifice plate blocking about 75 percent of the area operated stably with hydrogen to velocities as high as 280 feet per second at the same inlet air pressure and temperature. Temperature distribution downstream from an individual element tended to have a hot center core; more uniform distributions were obtained with V-gutter flame spreaders at the downstream end of the elements. The swirl-can elements also operated satisfactorily, at less severe conditions, with gaseous propane fuel.)

A quarter-annulus combustor with an array of these elements gave combustion efficiencies exceeding 85 percent in preliminary tests at a reference velocity of 180 feet per second, a pressure of 5.7 inches of mercury absolute, an inlet temperature of 350° F, and a combustor length of 13.5 inches. Total-pressure loss for this combustor was low; the outlet temperature distribution was initially unsatisfactory but was expected to improve with rearrangement of the combustor elements.

INTRODUCTION

Hydrogen used as a fuel for turbojet engines has shown promise of considerable increases in aircraft range; in addition, liquid hydrogen

CLASSIFICATION CHANGED
TO: UNCLASSIFIED
BY: AUTH. OF NASA HDQ. MEMO
NO 8-21-71, S.H. G. MAINES,
by C. L. F. 3-1-72

I.N. 11,394

MAY 14 1957

UNCLASSIFIED

N A C A LIBRARY

SECRET - LANGLEY AERONAUTICAL LABORATORY

Langley Field, Va.

~~CONFIDENTIAL~~

represents a large potential heat sink for airframe and engine cooling as might be required for very high flight speeds (refs. 1 and 2). Satisfactory combustion performance of hydrogen fuel at the very severe operating conditions encountered at high altitude has been demonstrated in full-scale turbojet engine tests (ref. 3). Finally, the use of this fuel may allow a major reduction in combustion-chamber length, enabling a saving in engine weight.

Experimental performance results have already been reported in the literature for a hydrogen-fuel turbojet combustor two-thirds the length of a conventional annular turbojet combustor (refs. 4 and 5). The shortening of the combustion chamber was accomplished by a reduction in the primary combustion-zone length; a substantial length was still required for mixing cold secondary air and the hot combustion gases for suitable turbine-inlet temperature profiles.

In a current research program conducted at the NACA Lewis laboratory, an alternative approach to turbojet combustor design is being explored which permits reductions in the secondary combustion-zone length as well as in the primary-zone length. In this design, the combustor is composed of a large number of similar elements which combine the functions of fuel injection, mixing, and flame stabilization. These elements are small cans within which rapid swirling mixes the fuel and air in a very short length. These individual swirl-can elements can be combined into a multiunit array covering the combustor cross section. The air necessary to complete the burning and reduce the temperature to the desired turbine-inlet temperature flows through the spaces between the combustor elements. This procedure results in many small cores of hot gas with a large interface area between the hot and cold streams. Rapid mixing can therefore be expected. This is in contrast to the usual combustor design where dilution air passing from an annulus into a single, large core of hot gases requires a relatively long length for adequate mixing.

This report presents the first phase of this research program. In this phase, the individual swirl-can elements that compose the combustor array are investigated. The isolated elements were operated with gaseous hydrogen in a one-twelfth sector of an annular turbojet combustor. Combustion efficiencies were investigated over a range of inlet total pressures from 5.7 to 14.7 inches of mercury absolute, reference velocities (based upon inlet conditions and maximum combustor cross section) from 75 to 180 feet per second, and a temperature of 350° F. These conditions included simulated operation of an engine with a compressor pressure ratio of 6.8 at altitudes from 70,000 to 90,000 feet at a Mach number of 0.9. Blowout limits were determined at combustor-inlet reference velocities up to 280 feet per second and total pressures as low as 4.0 inches of mercury absolute. Effects of geometry and fuel-injector position on the stability and combustion efficiency of the elements are described, and examples of

the exhaust temperature distribution downstream of the combustor are shown. Brief tests were also made with propane fuel for comparison purposes. In addition, preliminary results obtained with an array of several combustor elements in a quarter-annulus short combustor are presented.

SYMBOLS

A	area
G	mass flow rate per unit area
g_c	gravitational conversion factor
H	total enthalpy
P	pressure
R	specific gas constant
T	temperature, $^{\circ}\text{R}$
t	temperature, $^{\circ}\text{F}$
V	velocity, ft/sec
γ	ratio of specific heats

Subscripts:

B	combustor outlet
in	inlet
M	mass-weighted
ref	reference
s	static
t	total

APPARATUS

Installation

A schematic diagram of the combustor installation is shown in figure 1. Air of the desired quantity and pressure was drawn from the laboratory air supply system, metered with a sharp-edged orifice, passed through the combustor, and exhausted into the altitude exhaust system. Combustor-inlet temperatures were controlled by an inlet air heat exchanger supplied with hot exhaust gases from a gasoline-fired slave combustor. Airflow and combustion-chamber-inlet total pressure were regulated by remotely controlled valves with bypass lines and valves for fine adjustments.

The fuel supply system was similar to that used in previous research described in reference 5. The fuel was commercial hydrogen with a purity in excess of 99 percent. It was supplied in compressed-gas trailers at a maximum pressure of 2400 pounds per square inch. The fuel from the cylinders was reduced in pressure to 20 to 80 pounds per square inch gage, metered with a sharp-edged orifice, and then injected into the combustor.

The combustor test section consisted of a one-quarter sector of an annular combustor having an outside diameter of 25.5 inches and an inside diameter of 10.8 inches. This combustor housing was divided into three equal sectors by means of radial separation plates, each consisting of two parallel 0.06-inch walls separated by an air-cooled gap of 0.12 inch. With this arrangement, it was possible to investigate three different combustor elements simultaneously. The combustor cross-sectional area was 105 square inches for the one-quarter sector: each of the three one-twelfth sectors occupied approximately 32.7 square inches, and the balance was the blockage of the sector-dividing plates. A three-quarter view of the combustor is shown in figure 2 to illustrate the mounting of the combustor elements in the three independent sectors. A cross-sectional sketch of the combustor is shown in figure 3. The distance from the inlet of the combustor elements to the exhaust instrumentation plane was approximately 13.5 inches, depending upon the relative placement of the element with respect to the fuel supply tube.

A single-electrode spark wire provided ignition for starting the combustor elements. Each sector had its own ignition system, and the spark discharged directly to the downstream edge of each combustor element.

Combustor Instrumentation

The combustor instrumentation stations are shown in figure 1. At station 1 four bare-wire, Chromel-Alumel thermocouples, four total-pressure rakes, and a static-pressure tap measured the combustor-inlet

total temperature, total pressure, and static pressure, respectively. At station 2, a combined total-pressure and platinum-13-percent-rhodium - platinum aspirating-thermocouple probe in a polar-coordinate traversing mechanism (ref. 6) measured combustor-outlet total pressures and total temperatures. The probe moved circumferentially across all three sectors at five radial positions representing centers of equal annular areas. A two-pen X-Y recording potentiometer connected to the survey system recorded outlet temperatures and total-pressure drop across the combustor from stations 1 to 2. Static pressure was also measured at station 2 at duct wall taps.

Combustor Elements

The operation of a swirl-can combustor element is illustrated schematically in figure 4(a). Fuel was injected from a simple orifice at sonic velocity tangential to the inner surface and approximately normal to the axis of the can. The tangential velocity of the fuel caused the fuel to spiral downstream along the inside of the wall of the combustor element as verified by heat marks within the elements and observation of the flame through the periscope. Thus, the length of the average path travelled by the fuel stream through the combustor element was considerably greater than the axial distance from the fuel injector to the downstream edge of the element.

A cross-sectional view of a typical swirl-can combustor element is shown in figure 4(b). Each element consisted of a conical or a cylindrical shell; five sizes of conical shapes and three sizes of cylinders were investigated. A number of modifications to the inlets of the shells were tested to obtain the best combustion stability characteristics. Two configurations also were constructed with V-gutter flame spreaders at the outlet of the shell in an effort to improve outlet temperature distributions. Fuel was injected into the element through a spray bar with a 0.089-inch orifice; the spray-bar position was varied from 0.62 to 1.62 inches from the upstream edge of the element. The direction of fuel injection was varied from normal to the axis of the element to an angle of 40° in an upstream direction.

The combustor-element modifications investigated are listed and described in table I. The eight sizes of conical and cylindrical shells are designated by the letters A to H; the design modifications are designated by the numbers 0 to 11. Performance notes in table I will be discussed in the RESULTS and DISCUSSION sections.

PROCEDURE

Operating Conditions

The performance of the swirl-can combustor elements was investigated over a range of fuel-air ratios at the following inlet air conditions:

Total pressure, $P_{t,in}$, in. Hg abs	Airflow rate for quarter sector, lb/sec	Total temperature, $t_{t,in}$, °F	Reference velocity, V_{ref} , ft/sec (a)	Simulated altitude, ft	Severity factor, $\frac{V_{ref}}{P_{t,in} t_{t,in}}$, cu ft/(lb)(sec)(°R)
14.7	1.28	350	75	70,000	8.9×10^{-5}
9.0	.79	350	75	80,000	15
5.7	.51	350	75	90,000	23
5.7	.79	350	115	-----	35
5.7	1.28	350	180	-----	55

^aBased on combustor maximum cross-sectional area of 0.73 sq ft (quarter annulus) and combustor-inlet air density.

The first three conditions represent a present-day engine operating at a Mach number of 0.9 with an annular combustor and a compressor having a sea-level static total-pressure ratio of 6.8. The last two conditions were used to determine the performance of the combustors at higher velocities at the lowest pressure condition. The factor $V_{ref}/P_{t,in} t_{t,in}$ characterizes the severity of each operating condition. The parameter, derived from an analysis which assumes that the chemical reaction rate controls the combustion efficiency (ref. 7), has been used to correlate experimental combustion efficiency data. Generally, three different models were operated simultaneously at nearly identical conditions with data from all three of the models being recorded by the survey probe.

Calculations

Blowout limits. - Blowout of the combustor elements was observed visually through a periscope mounted upstream of the combustor as shown in figure 1. Blowout limits are reported in terms of the severity factor

at blowout $(V_{ref}/p_{t,in}T_{t,in})_{BO}$. Only the pressure and velocity were varied. Similar parameters of the type $p^{1.5}T/V$ (ref. 8) or V/pT (ref. 9) have been used by other investigators to establish approximate criteria for combustor blowout.

Combustion efficiency. - Combustion efficiency was calculated as the percentage ratio of actual to theoretical increase in enthalpy from the combustor-inlet instrumentation plane (station 1, fig. 1) to the combustor-outlet traversing plane (station 2, fig. 1) using the method of reference 10. Enthalpy values for hydrogen and its combustion products were obtained from references 11 and 12. A value of 51,571 Btu per pound was used for the lower heat of combustion of hydrogen.

Fuel and air flows to each of the three individual sectors of the combustor housing were not measured directly. The three combustor elements to be operated simultaneously in each run were matched to obtain equal effective fuel-orifice sizes and, consequently, equal fuel flows before installation in the combustor housing. As a first approximation, the air-flows to each sector were assumed equal. Combustion efficiency was then calculated from fuel-air ratio and enthalpy values based upon this mass-flow assumption. These combustion efficiencies were used to compare the performances of various configurations.

The performance of the most promising models was determined by means of a more precise method of calculation. This calculation required the determination of a mass-weighted combustor-outlet enthalpy and the actual mass flow through each combustor sector. The local mass-flow rate at any point in the combustor-outlet plane could be computed from the static pressure, total pressure, and total temperature by the following relation:

$$G = p_s \sqrt{\frac{2\gamma g_c}{(\gamma-1)RT_{t,B}} \left(\frac{p_{t,B}}{p_s}\right)^{\frac{\gamma-1}{\gamma}} \left[\left(\frac{p_{t,B}}{p_s}\right)^{\frac{\gamma-1}{\gamma}} - 1 \right]} \quad (1)$$

The exhaust-duct cross section was subdivided into 50 equal area increments ΔA for each one-twelfth sector. For each area increment, $p_{t,B}$ and $T_{t,B}$ were known from the continuous record of the exhaust survey probe, and the value of p_s measured at the wall tap was assumed constant across the duct. Accordingly, $p_{t,B}$, p_s , and $T_{t,B}$ were substituted into equation (1) to calculate G for each increment. The summation of all incremental airflows times the incremental area gave the total mass flow per sector.

The mass-weighted enthalpy H_M was defined by the summation

$$H_M = \frac{\sum HG \Delta A}{\sum G \Delta A} \quad (2)$$

where for each area increment the enthalpy H was determined from the local temperature and the enthalpy data for combustion products. Substituting equation (1) into equation (2) and assuming p , R , and γ to be approximately constant across the duct give

$$H_M = \frac{\sum H \left(\frac{p_{t,B}}{p_s} \right)^{\frac{\gamma-1}{2\gamma}} \sqrt{\frac{1}{T_{t,B}} \left[\left(\frac{p_{t,B}}{p_s} \right)^{\frac{\gamma-1}{\gamma}} - 1 \right]}}{\sum \left(\frac{p_{t,B}}{p_s} \right)^{\frac{\gamma-1}{2\gamma}} \sqrt{\frac{1}{T_{t,B}} \left[\left(\frac{p_{t,B}}{p_s} \right)^{\frac{\gamma-1}{\gamma}} - 1 \right]}} \quad (3)$$

RESULTS

A summary of the combustion performance characteristics of the different combustor elements investigated with hydrogen fuel is presented in table I. A brief description of the design modifications made and the purpose of the modification are noted in the table. The performance of each element is reported in table I in terms of (1) blowout severity factor $(V_{ref}/p_{t,in} T_{t,in})_{BO}$, (2) range of combustion efficiency for fuel-air ratios from 0.0016 to 0.0036 at a pressure of 5.7 inches of mercury absolute, a reference velocity of 75 feet per second, and an inlet temperature of 350° F, and (3) comments on the operation of the elements based on visual observation. Performance data for propane fuel are shown in table II for four of the better modifications.

Combustor Blowout

Stable operation was not obtained with a simple conical-shell element (model A0). As inlet blockage was increased, the stability defined by the blowout severity limit $(V_{ref}/p_{t,in} T_{t,in})_{BO}$ generally increased. Thus, stability was poorest for models A1 and A2 where inlet blockage was provided by a V-gutter extending across the inlet of the element. Since there was also a tendency for fuel to spill out of the V-gutter and the

inlet lip and burn outside the element, a ring was added to the inlet of model A2 to control this spillage. Increased blockage with the use of conical inlets (model B3) gave an improvement in stability limits. Further increases in stability were obtained by slotting the inlet cones (models A4 and B4), reducing the inlet-cone diameter (models A5 to B6), or twisting the serrations of the inlet cone to increase the turbulence level within the element (models A7 to A8). It was found, however, that the stability of the best conical inlet (model A8) could be duplicated by a much simpler modification consisting of a circular orifice plate blocking about 75 percent of the inlet area. The orifice-inlet configuration was investigated in a number of different basic shells (models A9 to E9). There appeared to be little difference in performance with respect to stability between the various conical shells, A to E, or the cylindrical shells, F to H. Excellent combustion stability was also obtained with an orifice-plate inlet with a blockage of only 65 percent (model A10).

In most cases, the severity factor at blowout decreased as fuel-air ratios were increased. This may be attributed to the fact that the elements operated at an internal fuel-air ratio above stoichiometric. For example, the internal fuel-air ratio for model B9 was calculated to be 40 times the over-all fuel-air ratio, neglecting the aerodynamic effects due to the burning within the element. For the over-all fuel-air ratio range of 0.0016 to 0.0032, calculated local fuel-air ratios for this model varied from 0.064 to 0.128. Thus, at severe conditions rich blowout might be expected, and it was not surprising that the configurations were slightly more stable at leaner fuel-air ratios. The effect of fuel-air ratio, however, was quite small and $(V_{ref}/p_{t,in} T_{t,in})_{BO}$ values presented in table I are average values obtained over a range of fuel-air ratios. Blowout was also determined at several mass flows; and, although the conditions at flame blowout were not entirely reproducible, the severity factors $(V_{ref}/p_{t,in} T_{t,in})_{BO}$ agreed to within 20 percent for different combinations of V_{ref} and $p_{t,in}$. Thus, the blowout severity factor of 87×10^{-5} for model B9 (table I) corresponded to blowout (at a constant inlet temperature of 350° F) at approximately 280 feet per second and a pressure of 5.7 inches of mercury absolute, or at 180 feet per second and a pressure of 3.6 inches of mercury absolute. In addition, the axial location of the fuel injector had little influence on combustion stability over the range of positions investigated. When the injector was located near the downstream end of the element, however, the fuel holes were drilled at an angle of 40° upstream of the normal to increase the residence time of the fuel in the element.

Propane stability data (table II) indicate that the selected elements can operate stably with this fuel, although blowout occurred at $(V_{ref}/p_{t,in} T_{t,in})_{BO}$ values 10 to 20 percent of the corresponding values for hydrogen. Best combustion stability was obtained with models B9 and B11.

Combustion Efficiency

Combustion efficiencies generally ranged from 80 to 90 percent for all the configurations at the conditions cited in table I. The efficiencies were calculated using area-average combustor-exhaust temperatures and the assumption that the mass flows through each combustor sector were equal. These values were sufficiently accurate to allow recognition of gross changes in performance accompanying the various design features. The combustion efficiency of three of the best models, B9, C9, and D9, however, was calculated using the incremental-area method expressed by equation (3). These elements ranged in inlet diameter from 0.93 (model C9) to 1.50 inches (model B9) and in length from 1.50 (model C9) to 2.00 inches (models B9 and D9). The smallest elements (model C9) were always operated in pairs to secure a coverage of the duct area comparable to that of the larger elements. Efficiencies are plotted against fuel-air ratio in figure 5 for four operating conditions. At the most severe condition (reference velocity, 180 ft/sec; pressure, 5.7 in. Hg abs; and inlet temperature, 350° F) the efficiency of models B9, C9, and D9 varied from 64 to 78 percent. At the conditions of lower reference velocities and higher pressures, efficiency levels improved appreciably. The effect of fuel-air ratio on combustion efficiency was not large. Combustion efficiency was not determined for propane operation with these three configurations, but, with model B11, combustion efficiencies of 86 to 100 percent were obtained with propane at the 14.7 inches of mercury pressure condition (fig. 5(d)).

Outlet Temperature Distribution

With the simultaneous operation of only three combustor elements within a quarter-annulus sector having a cross-sectional area of 105 square inches, a nonuniform outlet temperature distribution was to be expected. Two modifications, 6 and 11, incorporated V-gutter flame spreaders at the outlet of the element for the purpose of improving the outlet temperature distribution. Typical temperature profiles obtained with elements B9 without flame spreaders and B11 with flame spreaders at about the same fuel-air ratio are shown in figure 6. These profiles were constructed directly from the data recorded by the temperature survey probe by drawing constant-temperature contour curves between the recorded temperature-position data points. With model B11 the band of high temperatures is much broader, and the temperature-gradients are reduced.

Preliminary Performance of Multielement Combustor

A multielement combustor (fig. 7) consisting of five elements of model B11 at one radius and three elements of model B11 at a shorter

radius was constructed. This combustor was mounted in a quarter sector of an annular housing identical to that used in the study of the isolated elements, except that the radial separator plates were omitted. Each element had its own fuel injector supplied from a common manifold.

Brief tests were conducted with this combustor to demonstrate the feasibility of the multielement array. Combustion efficiencies were determined with hydrogen (fig. 8) at two reference velocities of 115 and 180 feet per second at an inlet total pressure of 5.7 inches of mercury absolute and an inlet total temperature of 350° F. At a velocity of 115 feet per second combustion efficiency varied from 92 to 97 percent, and, at the higher velocity, efficiency varied from 85 to 89 percent. The combustor was not operated with propane.

The distance from the upstream end of the combustor elements to the exhaust instrumentation plane was 13.5 inches, somewhat shorter than the corresponding length of 20 inches for the earlier quarter-annulus channelled-wall hydrogen combustor (ref. 5). Efficiencies with the latter combustor were of the order of 84 percent at conditions corresponding to a $V_{ref}/p_{t,in}T_{t,in}$ value of 52×10^{-5} cubic foot per pound-second-OR, compared with 85 to 89 percent for the multielement combustor at a $V_{ref}/p_{t,in}T_{t,in}$ of 55×10^{-5} .

A typical outlet temperature distribution obtained with this quarter-annulus combustor is shown in figure 9. The temperature gradients were rather steep radially with the highest temperatures at the midspan of the duct; circumferentially the hot gases were well distributed except near the side walls.

The isothermal pressure loss for this combustor was approximately 0.9 percent of the inlet total pressure at an inlet velocity of 75 feet per second, or about 4.5 times the inlet reference dynamic pressure.

DISCUSSION

Of the several geometry variables investigated, the amount of blockage at the inlet face of the combustor element had the largest effect on combustion stability. Best results were obtained with inlet area blockage as high as 75 percent; this was most easily accomplished with a flat plate having a circular orifice. For conical shells, increased inlet area blockage was also produced by a decreased inlet diameter. Where the orifice-plate inlet was installed, however, the amount of blockage at the inlet face provided by the plate was sufficiently great that changes in the inlet diameter of the element did not affect combustion stability. The position of the fuel injector within the element shell appeared to

have no effect on the stability of the element, provided the injector was not placed too close to the downstream end of the element thus allowing fuel to spill out too quickly.

From the 10 orifice-plate configurations, models B9, C9, D9, and B11 were arbitrarily selected for more extensive studies because these elements were conveniently sized for a proposed multielement combustor. These elements operated stably with hydrogen at conditions simulating operation of a present-day engine with a sea-level static compressor total-pressure ratio of 6.8 at a Mach number of 0.9 and altitudes of 70,000 to 90,000 feet. Even with the less-reactive propane fuel, stable operation was obtained at conditions simulating an altitude of 70,000 feet. Although these models were selected for expedience, it must also be noted that excellent performance was obtained with other configurations, particularly the cylindrical shells. A further investigation also may be warranted of other types of inlet blockage such as perforated plates, which have been shown to be very effective turbulence promoters and flame stabilizers (ref. 11).

The combustion efficiencies of the selected models, B9 to D9, are presented as a function of over-all fuel-air ratio in figure 5. This fuel-air ratio was based upon the entire mass flow through each combustor sector, and the values of this fuel-air ratio were considerably leaner than those expected with a full combustor. The airflow through each sector served only one isolated combustor element, whereas in a complete array three or more elements would occupy this space.

The combustion efficiency of the three selected models is plotted as a function of the parameter $V_{ref}/P_{t,in}T_{t,in}$ at a representative fuel-air ratio of 0.0030 in figure 10. The data were obtained from the faired curves of figure 5. As expected from previous experience with this parameter (ref. 7), combustion efficiency decreased with an increase in $V_{ref}/P_{t,in}T_{t,in}$. Model B9 gave somewhat higher efficiencies than the other two configurations. However, the spread among the efficiencies of the three models shown in figure 10 was probably less than the inaccuracy in the determination of combustion efficiency, since the nonuniform outlet temperature and pressure profiles introduced sampling errors.

The preliminary program with the quarter-annulus combustor used an array of model B11 elements with outlet V-gutter flame spreaders for control of temperature distributions. Combustion efficiencies with this combustor were higher than those obtained with the longer channeled-wall hydrogen combustor (ref. 5) at corresponding conditions. In addition, the isothermal total-pressure-loss for the multielement combustor was about 4.5 times the inlet reference dynamic pressure, a value considered more than satisfactory. The outlet temperature distribution (fig. 9) had

sharp radial gradients, but no effort was made to optimize this characteristic of the combustor. It is reasonable to expect that improvements in the temperature distribution can be brought about with small modifications in the array of elements.

No significant amount of warping or erosion of the swirl-can elements occurred during the course of the investigation, which accumulated more than 60 hours of operating time. The elements, however, were not operated for very long periods of time at high-temperature conditions. Visual observation of the elements through a periscope showed that the metal shells glowed red in some cases, indicating wall temperatures of perhaps 1200° to 1500° F. The elements operated cooler at higher fuel-air ratios because of the cooling effect of the fuel along the metal surfaces.

It is felt that the use of swirl-can combustor elements makes possible the design of a short-length, low-pressure-loss hydrogen combustor. The combustors appear to be adaptable to less-reactive vapor fuels such as propane if high combustion efficiency is not required at low pressures. Furthermore, the elemental, or modular, technique of constructing a turbojet combustor has the additional advantage of being a simple method of scaling from experimental combustor portions to full-scale annular combustors of any size.

SUMMARY OF RESULTS

The following results were obtained in an investigation of swirl-can combustor elements for a short-length, hydrogen-fuel turbojet combustor:

1. With 1.5- to 2.5-inch-diameter conical or cylindrical combustor elements, combustion efficiencies near 70 percent were attained at a reference velocity of 180 feet per second, a pressure of 5.7 inches of mercury absolute, and an inlet temperature of 350° F. These elements operated stably to velocities as high as 280 feet per second at the same inlet air pressure and temperature.

2. The combustor elements also operated satisfactorily with propane at less severe conditions at a reference velocity of 75 feet per second, a pressure of 14.7 inches of mercury absolute, and an inlet temperature of 350° F.

3. Exhaust temperature distributions from the combustor elements, while normally exhibiting a hot core of gases at the centerline of the element, were improved by the use of V-gutter flame spreaders at the outlet of the elements.

4. A 13.5-inch-long quarter-annulus combustor composed of an array of elements operated with combustion efficiencies of 85 to 89 percent at a reference velocity of 180 feet per second, a pressure of 5.7 inches of mercury absolute, and an inlet temperature of 350° F. The isothermal total-pressure drop was 0.9 percent of the combustor-inlet total pressure at a reference velocity of 75 feet per second and the same inlet air pressure and temperature. The outlet-temperature distribution was not satisfactory, but no work was done to optimize this aspect of the combustor performance.

Lewis Flight Propulsion Laboratory
National Advisory Committee for Aeronautics
Cleveland, Ohio, March 19, 1957

REFERENCES

1. Rothrock, Addison M.: Turbojet-Propulsion System Research and the Resulting Effects on Airplane Performance. NACA RM 54E23, 1955.
2. Silverstein, Abe, and Hall, Eldon W.: Liquid Hydrogen as a Jet Fuel for High-Altitude Aircraft. NACA RM E55C28a, 1955.
3. Fleming, W. A., Kaufman, H. R., Harp, J. L., Jr., and Chelko, L. J.: Turbojet Performance and Operation at High Altitudes with Hydrogen and JP-4 Fuels. NACA RM E56E14, 1956.
4. Sivo, Joseph N., and Fenn, David B.: Performance of a Short Combustor at High Altitudes Using Hydrogen Fuel. NACA RM E56D24, 1956.
5. Friedman, Robert, Norgren, Carl T., and Jones, Robert E.: Performance of a Short Turbojet Combustor with Hydrogen Fuel in a Quarter-Annulus Duct and Comparison with Performance in a Full-Scale Engine. NACA RM E56D16, 1956.
6. Friedman, Robert, and Carlson, Edward R.: A Polar-Coordinate Survey Method for Determining Jet-Engine-Combustion-Chamber Performance. NACA TN 3566, 1955.
7. Childs, J. Howard, and Graves, Charles C.: Relation of Turbine-Engine Combustion Efficiency to Second-Order Reaction Kinetics and Fundamental Flame Speed. NACA RM E54G23, 1954.
8. Schirmer, R. M., Kittredge, G. D., and Fromm, E. H.: Evaluation of Fuel Characteristics in Thermojet Engine Combustion Processes. Summary Rep. No. 403-19-52R, Phillips Petroleum Co., Jan. 1953. (Navy Contract NOas 52-132-C.)

9. Norgren, Carl T., and Childs, J. Howard: Effect of Fuel Injectors and Liner Design on Performance of an Annular Turbojet Combustor with Vapor Fuel. NACA RM E53B04, 1953.
10. Jonash, Edmund R., Smith, Arthur L., and Elavin, Vincent F.: Low-Pressure Performance of a Tubular Combustor with Gaseous Hydrogen. NACA RM E54L30a, 1955.
11. Keenan, Joseph H., and Kaye, Joseph: Gas Tables. John Wiley & Sons, Inc., 1948.
12. English, Robert E., and Hauser, Cavour H.: Thermodynamic Properties of Products of Combustion of Hydrogen with Air for Temperatures of 600° to 4400° R. NACA RM E56G03, 1956.
13. Haddock, Gordon W., and Childs, J. Howard: Preliminary Investigation of Combustion in Flowing Gas with Various Turbulence Promoters. NACA RM E8C02, 1948.

TABLE I. - SUMMARY OF DATA FOR INDIVIDUAL COMBUSTOR ELEMENTS WITH HYDROGEN FUEL

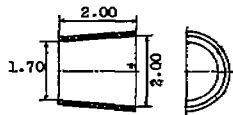
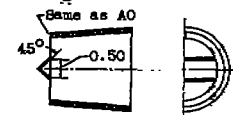
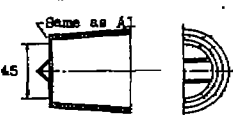
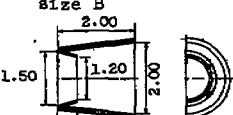
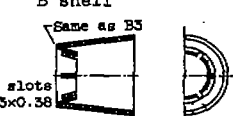
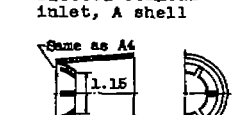
Model	Description and sketch of configuration (all dimensions in inches)	Purpose of modification	Blowout severity factor, $\left(\frac{V_{ref}}{P_t, in^T t, in / Bo}\right) \frac{cu ft}{(sec)(lb)(^{\circ}R)}$	Approximate range of combustion efficiency (at 5.7 in. Hg abs, 75 ft/sec, 350° F), percent	Comments on operation of combustor element
A0	Basic conical shell, Size A 	Original swirl can	-----	-----	No stable operation could be maintained.
A1	V-gutter inlet Same as A0 	V-gutter placed across inlet to element shell to increase stability by creating stable piloting region within V-gutter	37×10^{-5}	80 to 90	Operation poor; fuel tended to spill out of V-gutter and element inlet and burn outside element.
A2	V-gutter inlet and ring Same as A1 	Small ring added around inlet to reduce fuel spillage experienced with model A1	33×10^{-5}	80 to 90	Very little reduction in fuel spillage. Operation was apparently inferior to that with A1, and use of inlet V-gutters was abandoned.
B3	Conical inlet with basic conical shell, size B 	Inlet blockage provided by conical inlet, which created low-velocity region around cone	38×10^{-5}	~80	Element was very sensitive to fuel-air ratio. Inlet blockage was apparently insufficient.
A4	Slotted conical inlet, A shell Same as A0 Six slots 0.13 x 0.38 	Slots cut into inlet cone to increase turbulence	24×10^{-5}	-----	Stability was poor.
B4	Slotted conical inlet, B shell Same as B3 Six slots 0.13 x 0.38 	Same as A4, with B size shell	35×10^{-5}	~80	Stability was somewhat better because of the increased inlet blockage of shell B.
A5	Reduced-diameter slotted conical inlet, A shell Same as A4 	Frontal blockage increased with smaller-diameter inlet cone, while retaining advantages of slots.	38×10^{-5}	75 to 85	Fair stability, representing improvement over that of A4

TABLE I. - Continued. SUMMARY OF DATA FOR INDIVIDUAL COMBUSTOR ELEMENTS WITH HYDROGEN FUEL

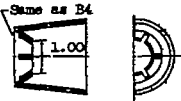
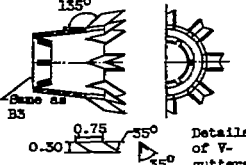
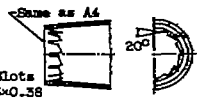
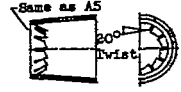
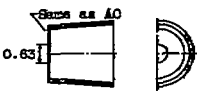
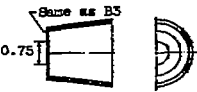
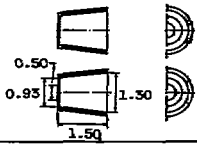
Model	Description and sketch of configuration (all dimensions in inches except where noted)	Purpose of modification	Blowout severity factor, $\left(\frac{V_{ref}}{\sqrt{Pt, in^T, in/B_0}}\right) \frac{cu ft}{(sec)(lb)(^{\circ}R)}$	Approximate range of combustion efficiency (at 5.7 in. Hg abs, 75 ft/sec, 350° F), percent	Comments on operation of combustor element
B5	Reduced-diameter slotted conical inlet, B shell 	Same as A5, with B size shell	45×10^{-5}	~85	Advantages of reduced-diameter inlet also evident in B size shell.
B6	Reduced-diameter slotted conical inlet with outlet V-gutter flame spreaders 	Eight V-gutter flame spreaders, sloping outward at 45°, added to outlet of B5 to improve outlet temperature distribution	66×10^{-5}	~85	Flame spreaders had favorable influence on outlet temperature distribution as discussed in text. Improvement in stability was also noted.
A7	Twisted serrated conical inlet, A shell 	Slotted inlet of A4 further slotted and remaining metal tabs twisted to increase flameholding surfaces and create additional turbulence at inlet	51×10^{-5}	80 to 90	Good stability.
A8	Reduced-diameter twisted, serrated conical inlet 	Frontal blockage reduced with smaller-diameter cone, using inlet of model A7	68×10^{-5}	80 to 90	Further improved stability over that of A7
A9	Orifice inlet, with basic conical shell, size A 	Simple orifice plates used as inlet modification instead of cones to provide the required blockage. Orifice opening ranged from 0.19 to 0.29 percent of inlet area.	87×10^{-5}	85 to 92	Exceptionally stable. Orifice-inlet models proved to be the most successful in regard to blowout limits and operation over a wide range of fuel-air ratios and represented a design simplification over models A7, A8, etc.
B9	Orifice inlet, with basic conical shell, size B 	Orifice inlet installed in B conical shell, which had slightly smaller inlet diameter than A shell	87×10^{-5}	93 to 100 (More complete data shown in fig. 5(a))	Approximately same performance as A9
C9	Orifice inlet, with basic conical shell, size C 	Orifice inlet installed in C conical shell, which was smaller in length and diameter than A or B shell and was operated in pairs	72×10^{-5}	90 to 99 (More complete data shown in fig. 5(b))	Approximately same performance as A9

TABLE I. - Concluded. SUMMARY OF DATA FOR INDIVIDUAL COMBUSTOR ELEMENTS WITH HYDROGEN FUEL

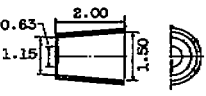
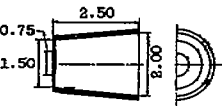
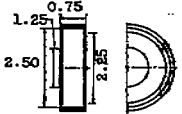
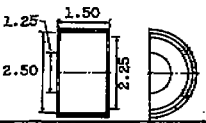
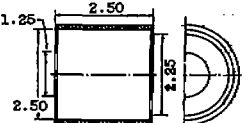
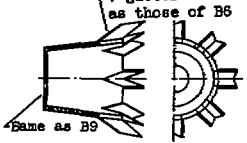
Model	Description and sketch of configuration (all dimensions in inches)	Purpose of modification	Blowout severity factor, $\left(\frac{V_{ref}}{p_t, in^2, in/B_0}\right)$ $\frac{cu ft}{(sec)(lb)(OR)}$	Approximate range of combustion efficiency (at 5.7 in. Hg abs, 75 ft/sec, 350° F), percent	Comments on operation of combustor element
D9	Orifice inlet, with basic conical shell, size D 	Orifice inlet installed in D conical shell, which was equal to A and B in length but smaller in both inlet and outlet diameter	96×10^{-5}	86 to 99 (More complete data shown in Fig. 5(c))	Approximately same performance as A9
E9	Orifice inlet, with basic conical shell, size E 	Orifice inlet installed in E conical shell, which was equal to B in inlet and outlet diameter but longer	89×10^{-5}	85 to 95	Approximately same performance as A9 although model tended to blow out at rich fuel-air ratios
F9	Orifice inlet, with basic cylindrical shell, size F 	Same as A9 to E9, but in cylindrical shells; shell F shortest in length	84×10^{-5}	80 to 90	Approximately same performance as A9
G9	Orifice inlet, with basic cylindrical shell, size G 	Orifice inlet installed in G cylindrical shell, which was equivalent to F in diameter but longer	92×10^{-5}	80 to 90	Approximately same performance as A9
H9	Orifice inlet, with basic cylindrical shell, size H 	Orifice inlet installed in H cylindrical shell, which was equivalent to G in diameter but longer	84×10^{-5}	80 to 90	Approximately same performance as A9
A10	Orifice inlet with larger opening Same as A0 	Large orifice opening (area ratio, 0.35) used to determine if decreased inlet blockage would give satisfactory results	80×10^{-5}	85 to 92	Over the limited range of orifice-area ratios investigated, this blockage change did not appear to affect performance of elements.
B11	Orifice inlet with outlet V-gutter flame spreaders V-gutters same as those of B8 Same as B9 	Eight V-gutter flame spreaders added to outlet of B9 to improve outlet temperature distribution	-----	-----	Operated mainly with propane. Same improvement in outlet temperature distribution with V-gutter flame spreaders as was noted with B8

TABLE II. - SUMMARY OF DATA FOR INDIVIDUAL
COMBUSTOR ELEMENTS WITH PROPANE FUEL

Model designation	Blowout severity factor, $\left(\frac{V_{ref}}{P_{t,in} T_{t,in}} \right)_{BO}$ cu ft (sec)(lb)(°R)	Approximate range of combustion efficiency (at 14.7 in. Hg abs, 75 ft/sec, 350° F), percent
B9	13x10 ⁻⁵	(Not determined)
C9	9.3	(Not determined)
D9	7.7	(Not determined)
B11	15	86 to 100

4390

CC-3 back

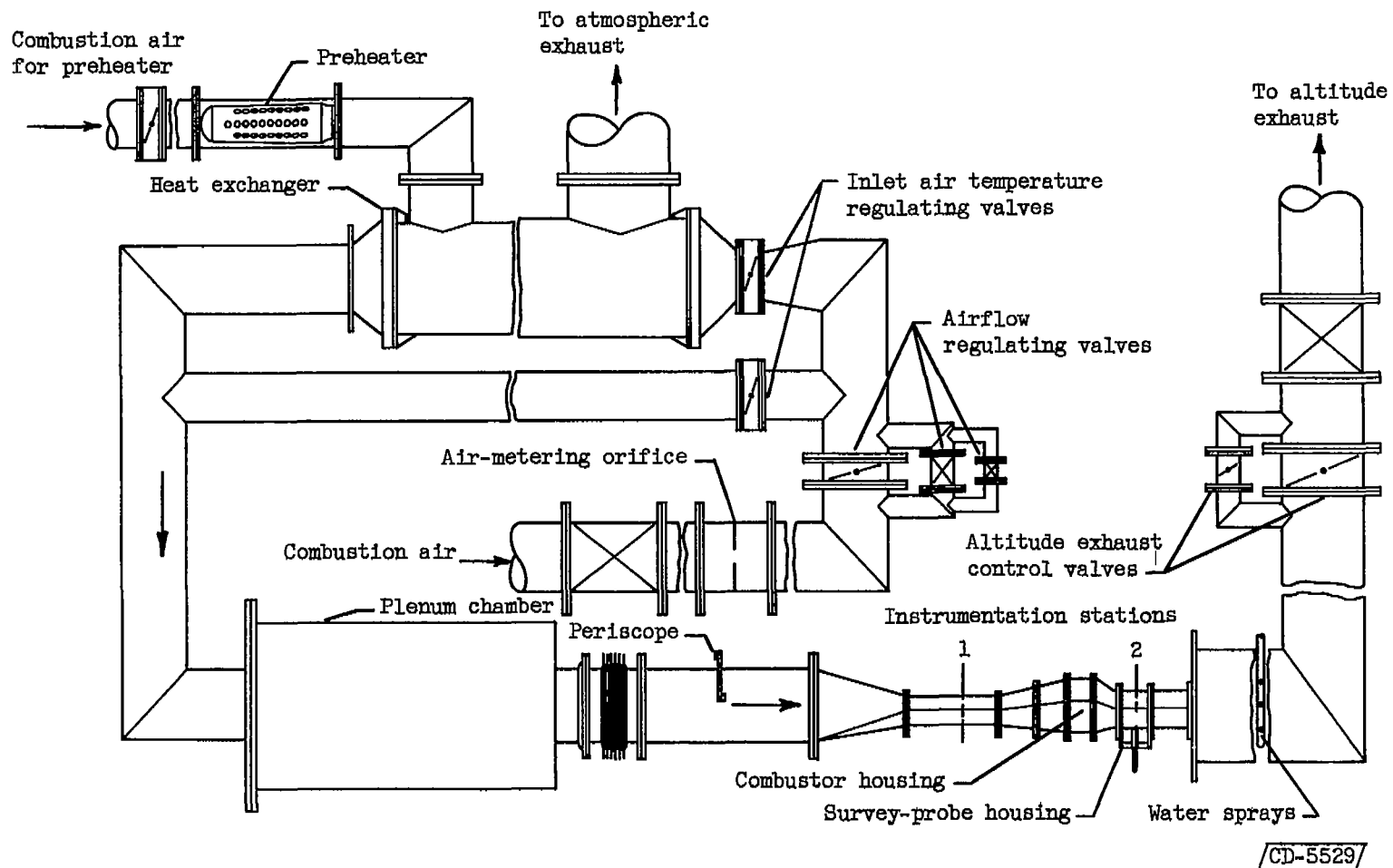


Figure 1. - Installation of experimental quarter-annulus combustor housing for investigation of individual combustor elements.

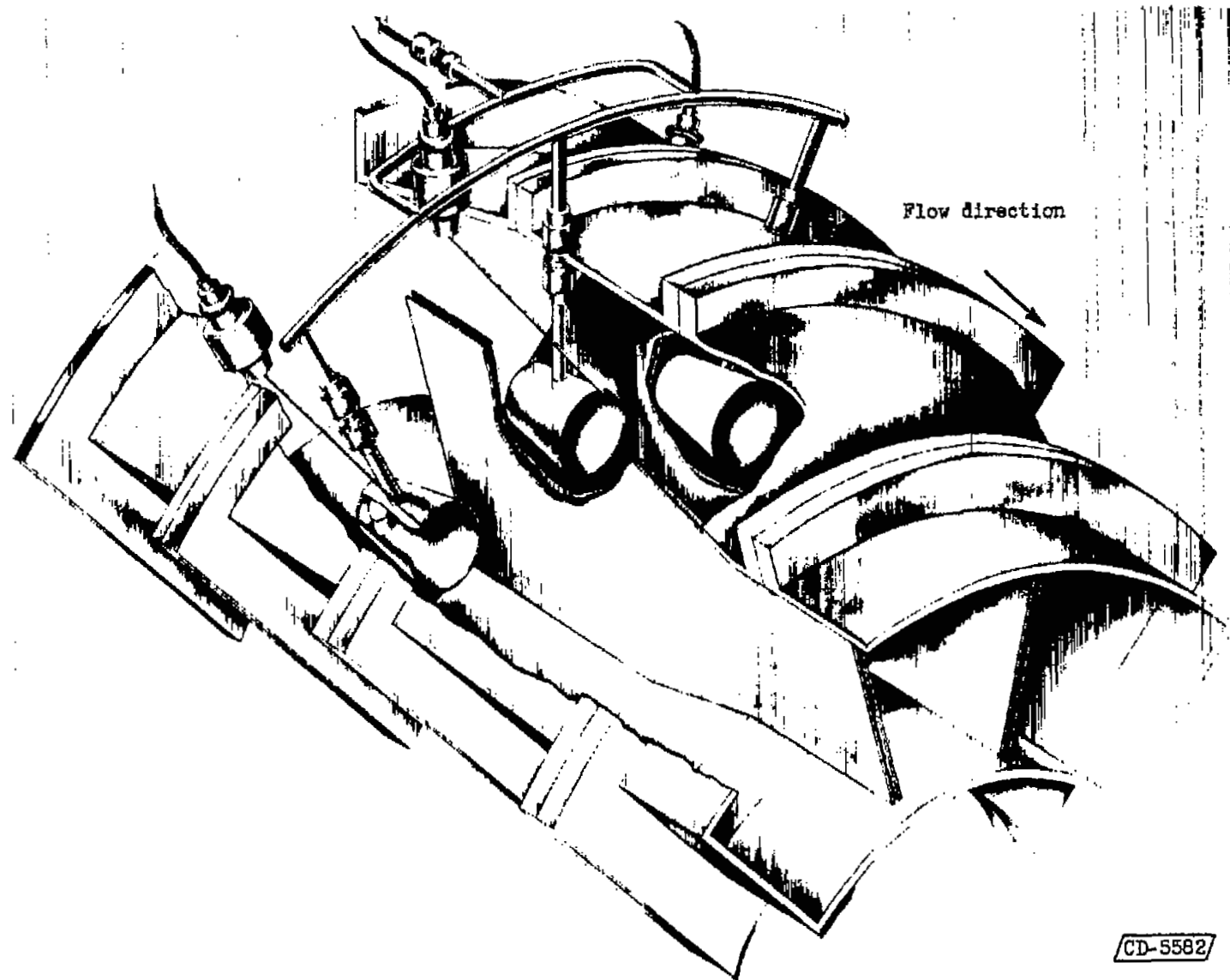


Figure 2. - Three-quarter cutaway view of quarter-annulus combustor housing showing mounting of three combustor elements for simultaneous operation.

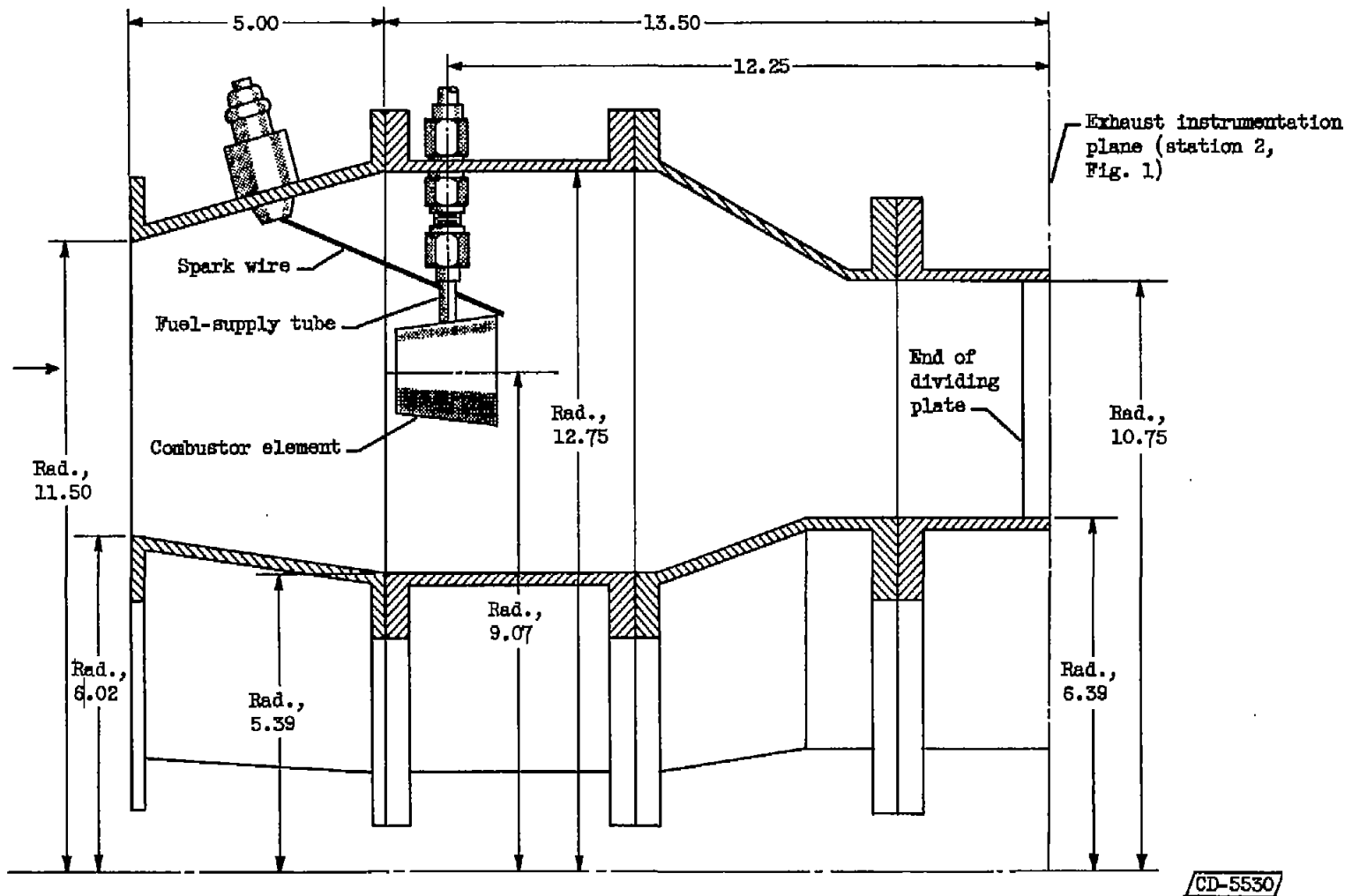
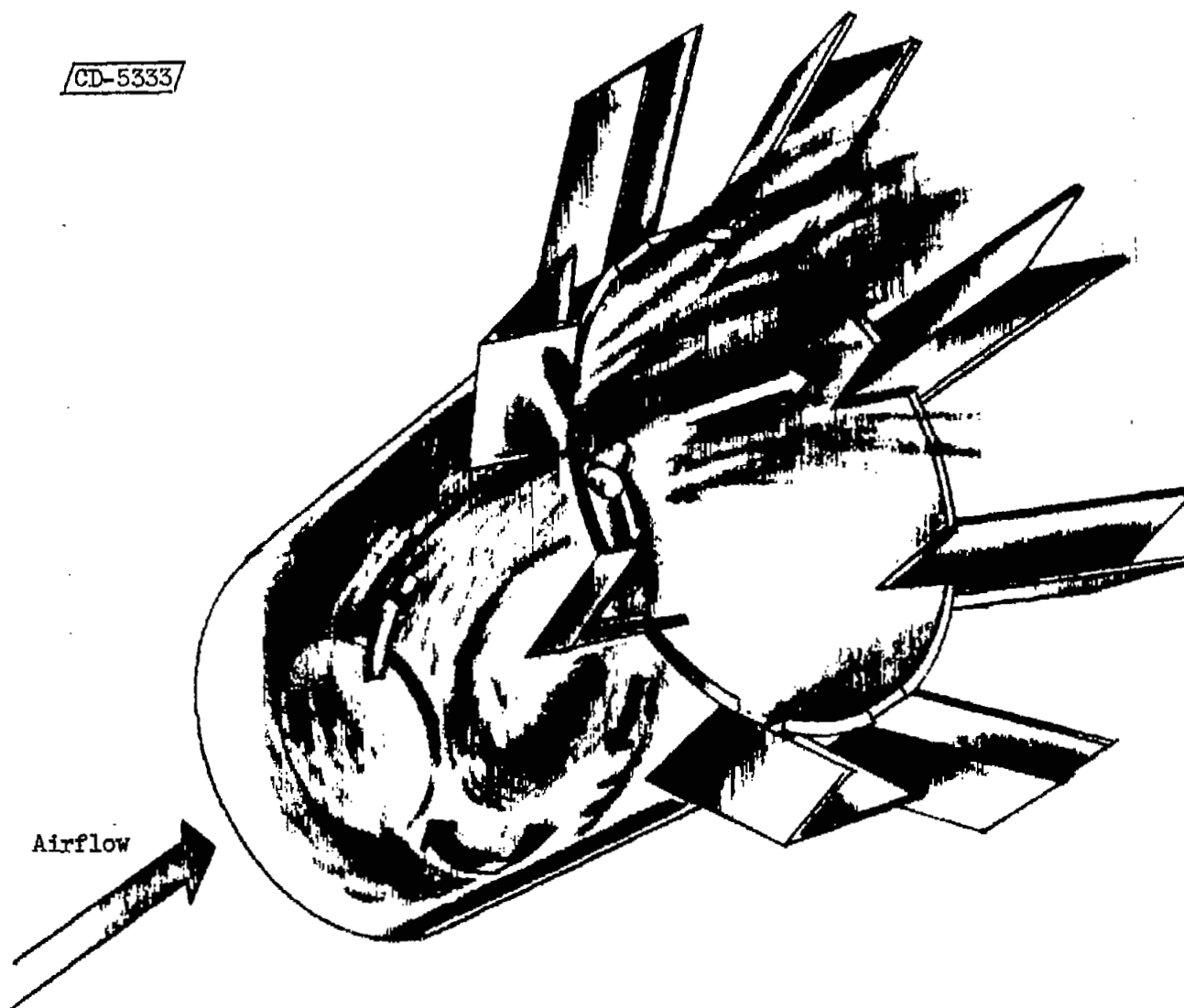
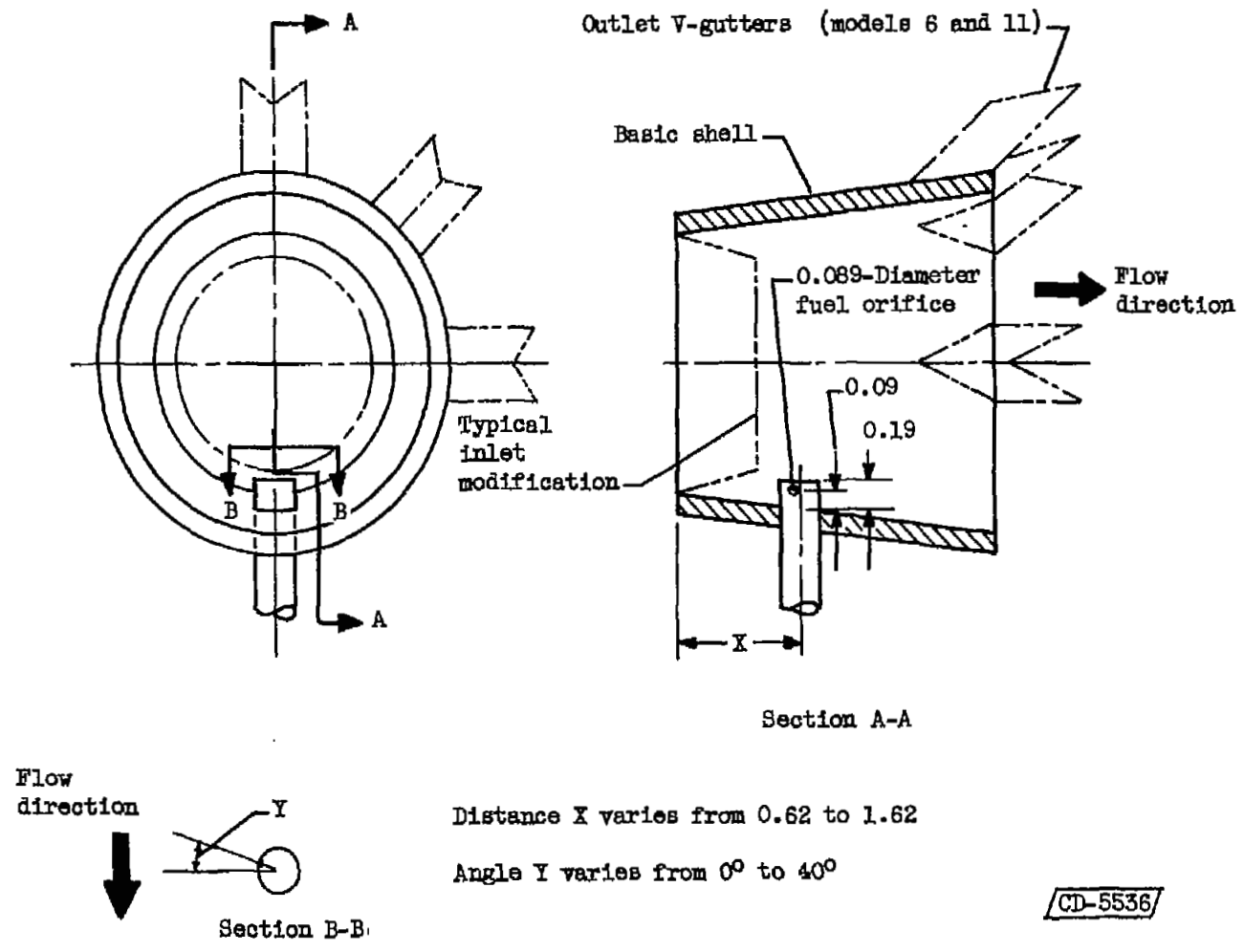


Figure 3. - Cross section of quarter-annulus combustor housing. Combustor maximum cross-sectional area, 0.75 square foot. (All dimensions in inches.)



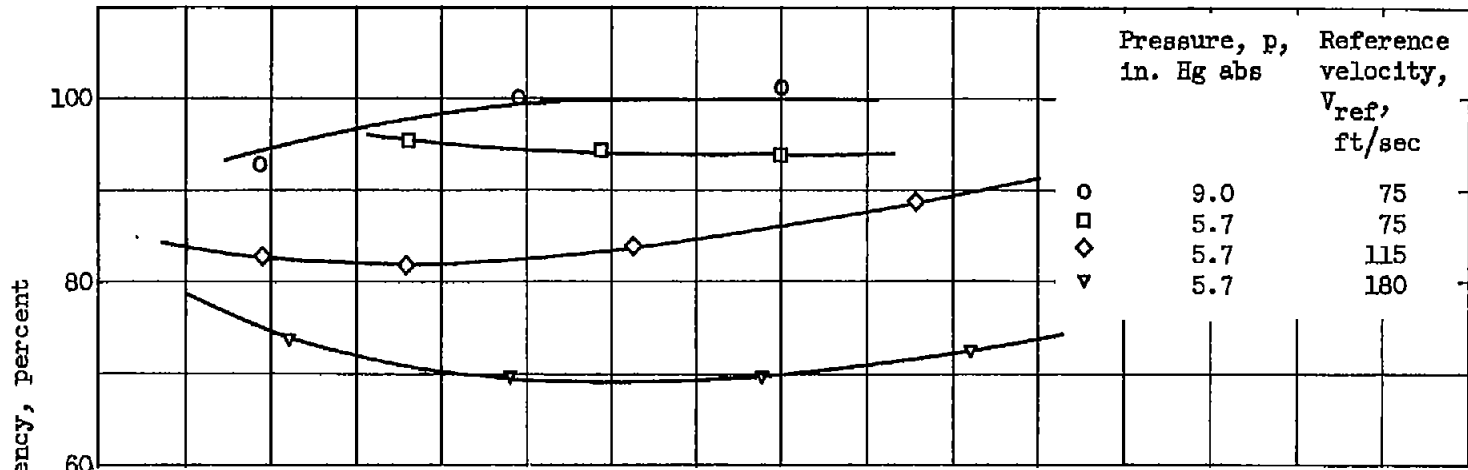
(a) Pictorial view of operation of typical swirl-can combustor element (model B11).

Figure 4. - Typical combustor element. (See table I for principal dimensions.)

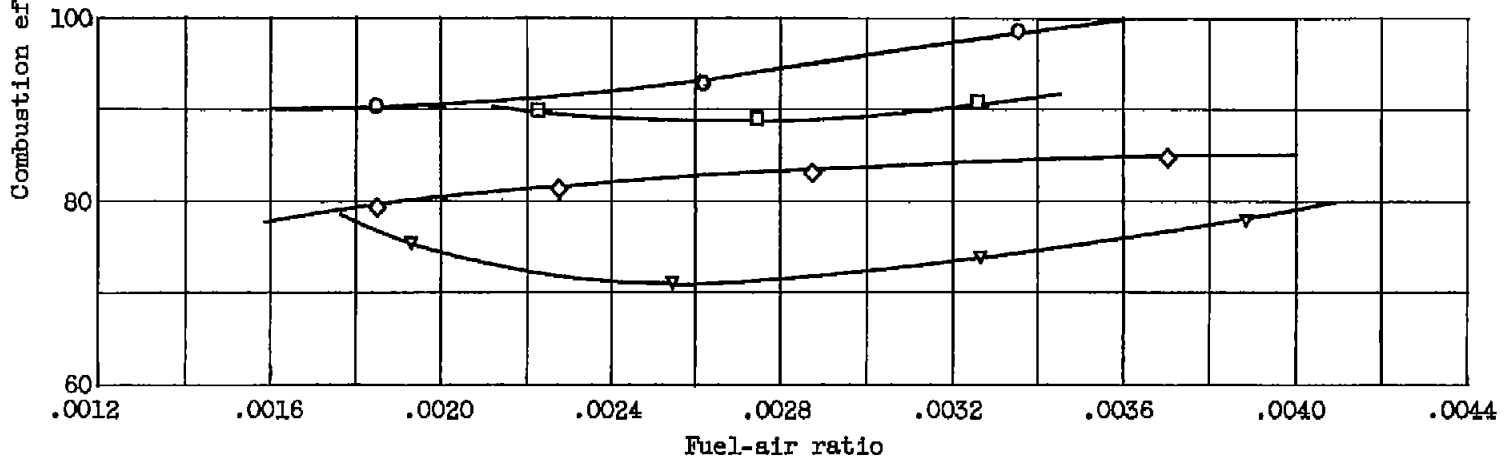


(b) Cross section. (All dimensions in inches.)

Figure 4. - Concluded. Typical combustor elements. (See table I for principal dimensions.)

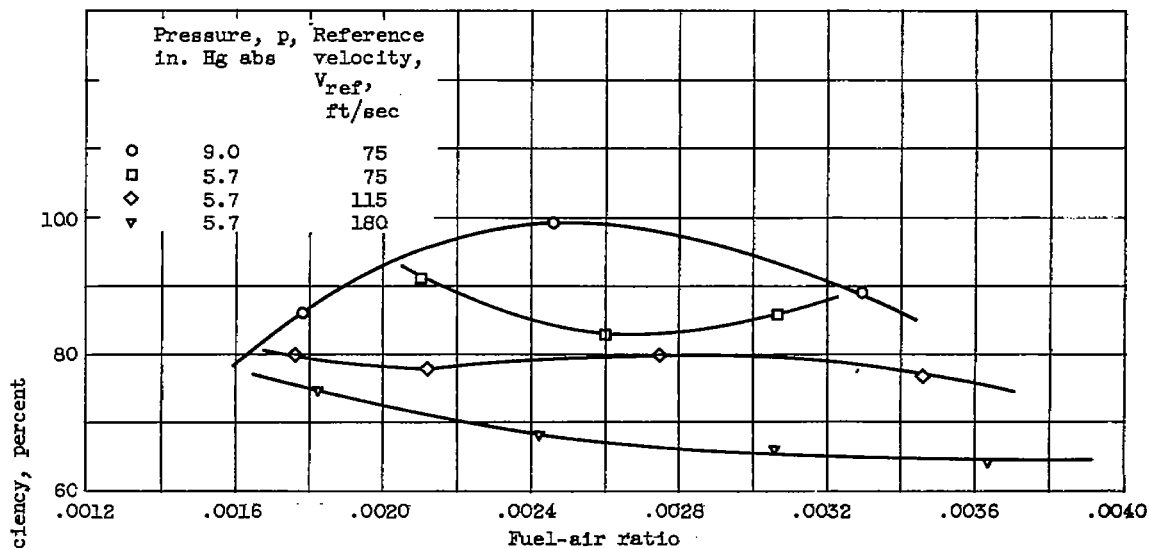


(a) Model B9. Efficiency calculated using incremental-area method.

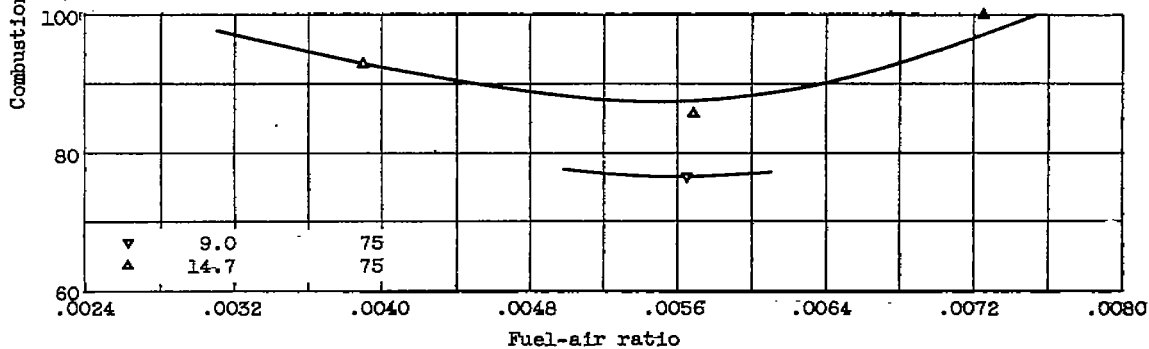


(b) Model C9. Efficiency calculated using incremental-area method.

Figure 5. - Combustion efficiency of selected combustor elements with orifice inlets. Inlet temperature, 350° F.

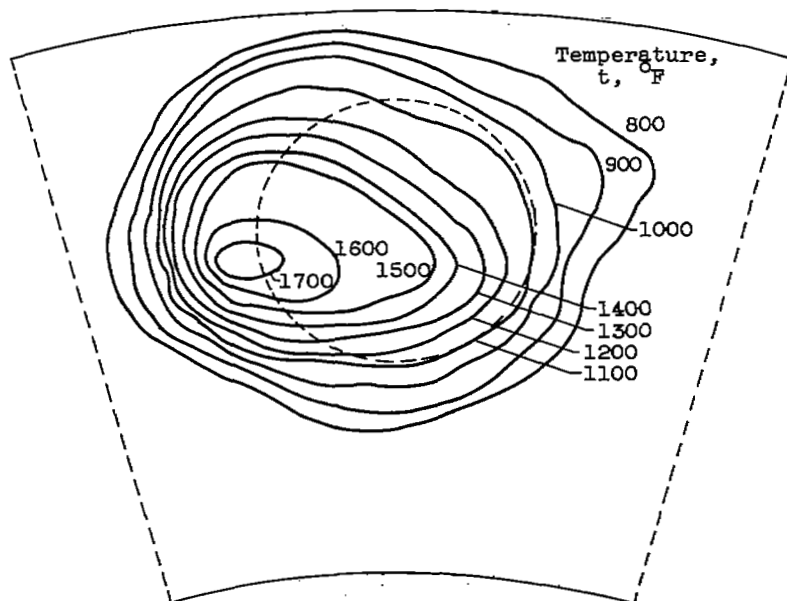


(c) Model D9. Efficiency calculated using incremental-area method.

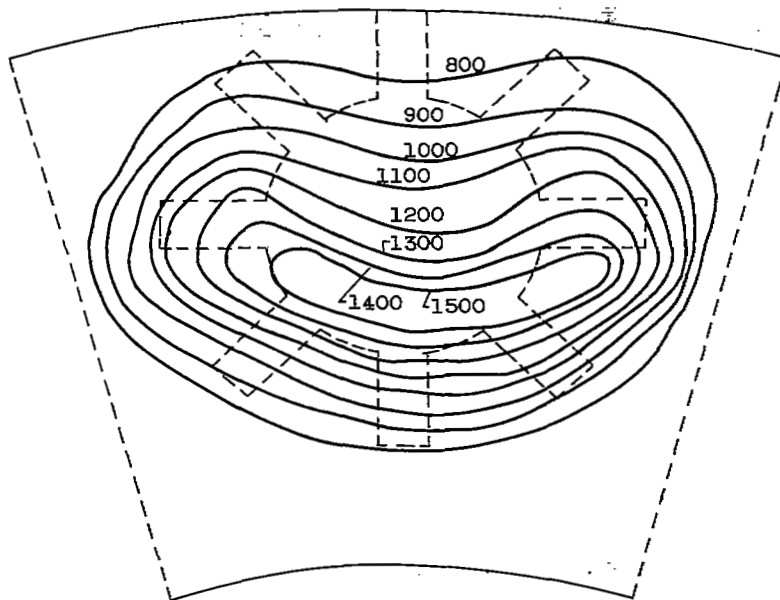


(d) Model B11 with propane. Efficiency calculated using area-averaged combustor-exhaust temperatures.

Figure 5. - Concluded. Combustion efficiency of selected combustor elements with orifice inlets. Inlet temperature, 350° F.



(a) Typical temperature distribution from model B9 without outlet flame spreaders.

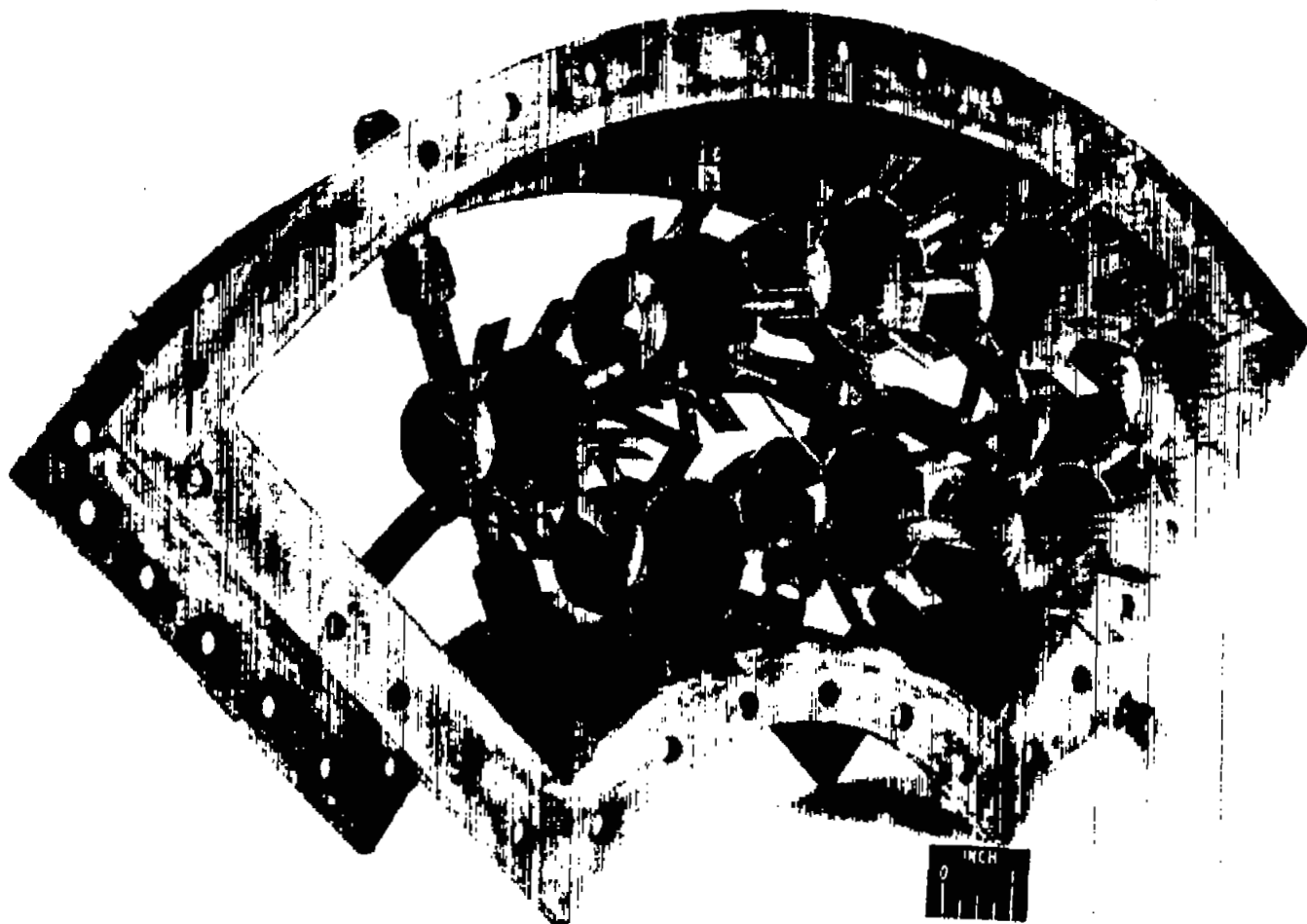


(b) Typical temperature distribution from model B11 with outlet flame spreaders.

Figure 6. - Temperature contours 13.5 inches downstream of single combustor elements. Combustor-inlet pressure, 5.7 inches of mercury absolute; combustor-inlet temperature, 350° F; reference velocity, 75 feet per second; fuel-air ratio, 0.0025. Location of downstream edge of element shown by broken lines.

4390

QC-4 back



C-42764

Figure 7. - Photograph of quarter-annulus combustor composed of an array of model B11 combustor elements.

4390

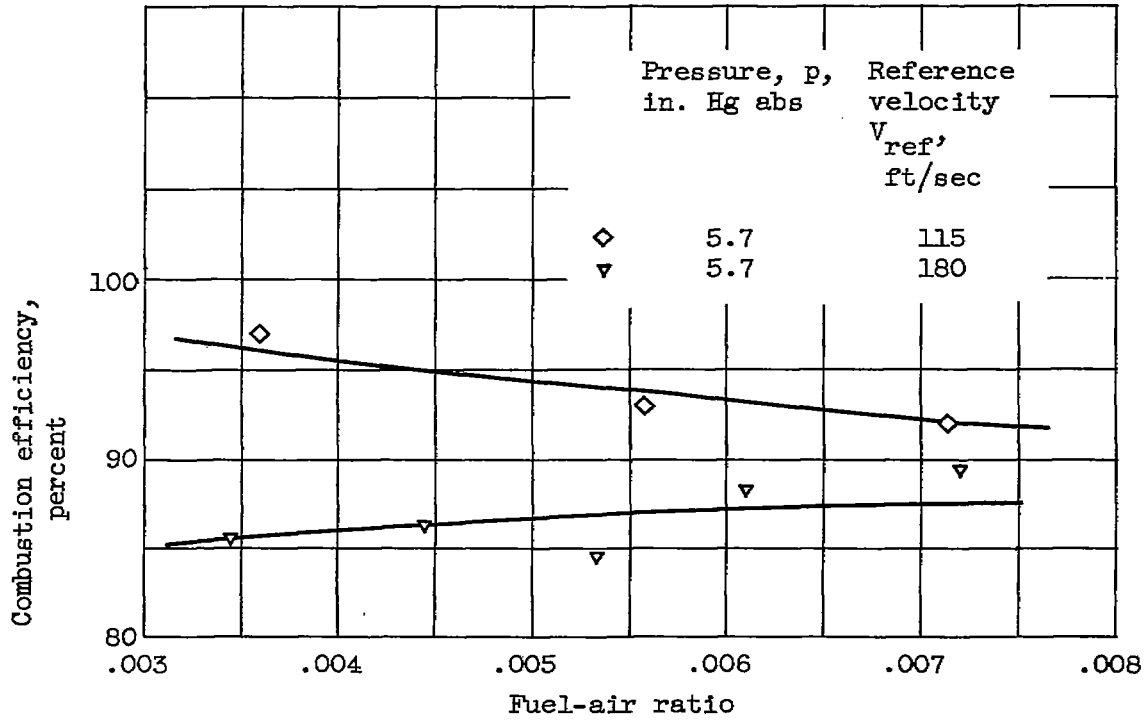


Figure 8. - Combustion efficiency of a quarter-annulus combustor composed of an array of eight model B11 combustor elements. Inlet temperature, 350° F.

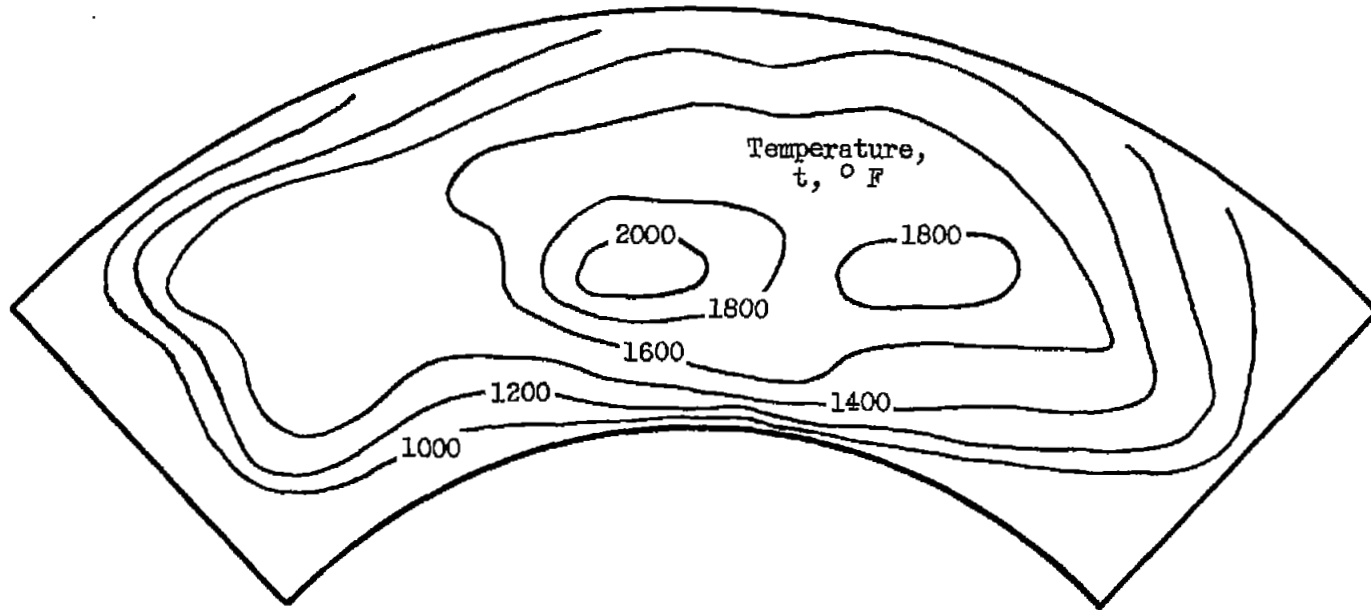


Figure 9. - Temperature contours 13.5 inches downstream of quarter-annulus combustor composed of an array of eight combustor elements. Combustor-inlet pressure, 5.7 inches of mercury absolute; combustor-inlet temperature, $350^\circ F$; reference velocity, 75 feet per second; fuel-air ratio, 0.0064.

UNCLASSIFIED

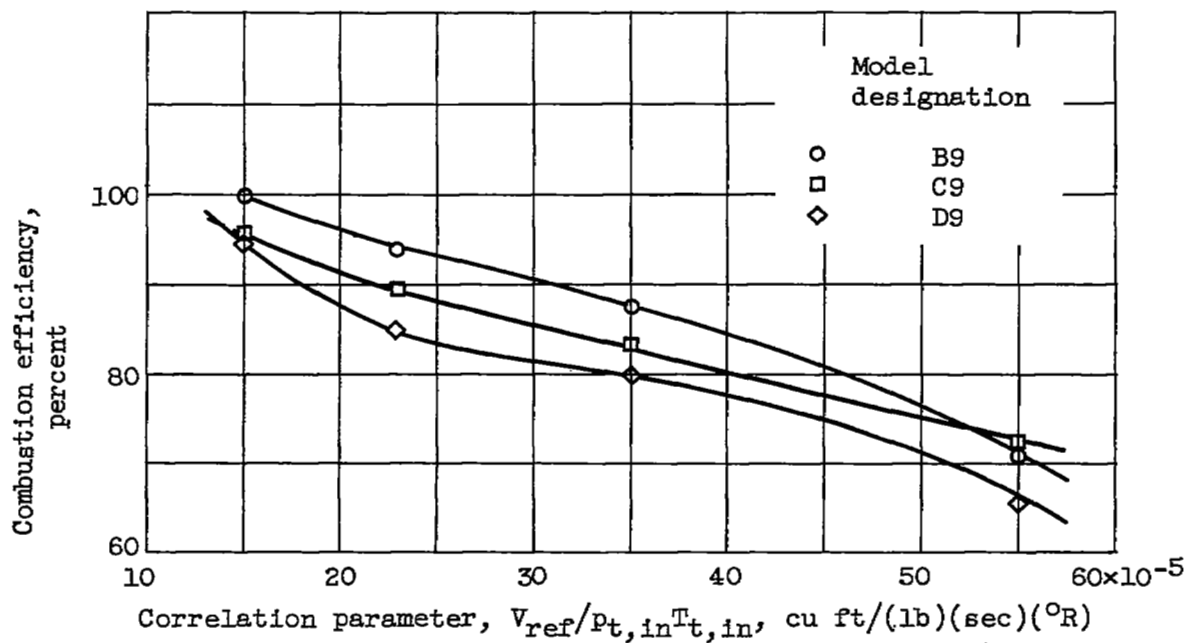


Figure 10. - Combustion efficiency of three selected orifice-inlet combustor elements as function of correlation parameter. Fuel-air ratio, 0.0030.

UNCLASSIFIED



3 1176 01436 5796

UNCLASSIFIED

UNCLASSIFIED

~~CONFIDENTIAL~~